ACTA GEOLOGICA HISPANICA, v. 32 (1997), nº 3-4, p. 201-219 (Pub. 1999)

Paleomagnetism and astronomically induced cyclicity of the Armantes section; a Miocene continental red bed sequence in the Calatayud-Daroca basin (Central Spain)

Paleomagnetismo y ciclicidad astronómica en los sedimentos aluviales de la sucesión de Armantes (Cuenca de Calatayud-Daroca, Cordillera Ibérica)

W. KRIJGSMAN[1], W. DELAHAIJE[1], C.G. LANGEREIS[1] and P.L. DE BOER[2]

(1)Paleomagnetic Laboratory, Fort Hoofddijk, Budapestlaan 17, 3584 CD Utrecht, The Netherlands. e-mail: krijgsma@geo.uu.nl

(2)Dept. of Geology, Institute of Earth Sciences, Budapestlaan 4, 3584 CD Utrecht, The Netherlands

ABSTRACT

The Armantes section is a red-bed sequence consisting of a regular alternation (10 m scale) of reddish silts and pink/white limestones. In between these limestones, a smaller-scale bedding (2-3 m scale) is intercalated, characterised by varying carbonate content and related differences in erosion resistance. An earlier correlation of the magnetic polarity sequence of the Armantes section to the geomagnetic polarity time scale (GPTS) suggested a periodicity of 111 kyr for the large-scale cyclicity (Krijgsman et al., 1994b). The carbonate, gamma-ray and susceptibility records indicate that 4 to 5 small-scale cycles are developed in one large-scale cycle, showing that the small-scale cyclicity is related to precession and thus caused by climate forcing. We suggest that the precipitation of the carbonates is most likely related to rising ground-water levels and an increase of evaporation. This implies that the thick limestone beds would correlate to eccentricity maxima and the smaller-scale limestone beds to precession minima. Rock magnetic experiments show that the NRM in the Armantes section results from the presence of hematite and magnetite/maghemite. The relative contribution of hematite is strongly related to the lithology. Hematite is the dominant carrier in the limestones, while in the silts magnetite/maghemite prevail.

Keywords: Paleomagnetism. Magnetostratigraphy. Cyclicity. Red beds. Miocene. Spain.

RESUMEN

La sucesión de Armantes tiene una potencia de cerca de 300 metros de sedimentos lutíticos depositados en un medio aluvial distal. Éstos consisten en una alternancia regular decamétrica de lutitas rojas y calizas blanco-rosadas. Las calizas contienen a su vez estratos de escala menor (2-3 metros) con un contenido variable de carbonato, característica que se ve reflejada en las diferentes resistencias a la erosión de estratos consecutivos. La correlación magnetoestratigráfica de la sucesión de Armantes con la escala de tiempo de polari-

dad magnética indica una periodicidad de 111 kyr para la ciclicidad de mayor escala (Krijgsman et al., 1994b), que sugiere una correspondencia con el periodo de ~100 kyr de excentricidad de la órbita terrestre. A partir de los valores de contenido en carbonato, rayos gamma y susceptibilidad magnética se observa que dentro de cada uno de los ciclos de mayor escala se definen de 4 a 5 ciclos de menor escala. Esto muestra que la ciclicidad de pequeña escala está relacionada con la precesión y, por tanto, es de origen climático. Se sugiere que la precipitación de carbonato está probablemente relacionada con una elevación del nivel freático y a un incremento en la tasa de evaporación, lo que sugiere que los estratos de caliza más potentes se correlacionarían con máximos de excentricidad, y las capas delgadas de calizas con mínimos de precesión. El estudio de las propiedades magnéticas de los sedimentos indica que la magnetización remanente natural en la sucesión de Armantes es resultado de la presencia de hematites y magnetita/maghemita. La contribución relativa de estos minerales está estrechamente ligada a la litología. En las calizas el principal mineral portador de magnetización es la hematites, mientras que en los limos la contribución de magnetita/maghemita es más importante.

Palabras clave: Paleomagnetismo. Magnetoestratigrafía. Ciclicidad. *Red beds*. Mioceno. España.

INTRODUCTION

Time is an indispensible tool in geology for constraining all kinds of processes and rates of change. A major break-through in chronology - with a resolution and accuracy of several kyr - recently came from marine studies directed at establishing an astronomical polarity time scale (APTS) (Shackleton et al., 1990, 1995; Hilgen 1991a,b, Hilgen et al., 1995). The construction of such a time scale involves the calibration (or "tuning") of astronomically induced sedimentary cycles or other cyclic variations in sedimentary sequences to computed astronomical time series of past variations in the Earth's orbit or to derived target curves (e.g. insolation, ice sheet volume). For paleoclimate and paleoenvironment reconstructions, the APTS is fundamental, but the construction of the APTS is, as yet, entirely based on open- marine sequences. The inclusion of the continental record would be forwarding since a comprehensive understanding of paleoclimate and paleoclimate change is only achieved by accurate and high-resolution time-stratigraphic correlations between the continental and the marine record. In fact, the terrestrial sedimentary record seems to be the logical place to look for Milankovitch cycles because, in the absence of oceanographic processes with their intrinsic and complicated non-linear (feed-back) mechanisms, a more direct registration of orbitally induced changes of climate may be expected (De Boer and Smith, 1994).

A potential and serious drawback from using continental successions is the usual lack of a direct and sufficient time control, also because of the assumed common occurrence of hiatuses which may result from intermittent erosion caused by tectonic activity, base-level changes and autocyclic processes. High-resolution magnetostratigraphic studies on continental sections in the Calatayud-Daroca basin of Spain, however, showed that a continuous sedimentation - without major hiatuses - has taken place during the Miocene, providing accurate time constraints (Krijgsman et al., 1994b; 1996). The mammal biostratigraphic record of these sections is extremely dense and rich, and offers a resolution of 30 kyr for some intervals. The series ranges from the Neogene Mammal zone MN 4 (18 Ma; Aragonian) to MN 11 (8 Ma; Turolian) (Krijgsman et al., 1994b; 1996). Principal component analyses of the detailed rodent assemblages from the Ramblian and Aragonian (Van der Meulen and Daams, 1992) revealed that major climate changes can be recognised in the continental biostratigraphic record in Spain. The construction of an APTS in the Calatayud-Daroca basin will allow the incorporation of this part of the continental record in a global and astronomically tuned cyclostratigraphic and magnetostratigraphic framework. This, in turn, will allow the establishment of high-resolution time-stratigraphic correlations between the continental and the marine record nèeded for a comprehensive understanding of paleoclimate and paleoclimate change.

Sections with a continuous cyclic sedimentation pattern and good paleomagnetic properties are needed for investigating the potential of constructing an APTS. For this study, we selected the Armantes section, a typical example of a red bed sequence. Correlation of the Armantes magnetic polarity sequence to the geomagnetic polarity time scale CK95 of Cande and Kent (1995) showed that sedimentation has been continuous over a 5 Myr interval (Krijgsman et al. 1994b). A 10 m scale cyclic bedding of alternating reddish silts (red beds) and whitish limestones is very pronounced and, in addition, smaller-scale (2-3 m) variations in lithology are expressed as a laterally continuous alternation of slightly more and slightly less erosion-resistent siltstones. The magnetostratigraphic results further showed that the 10 m scale cyclic bedding has an average periodicity of 111 kyr (27 cycles in 3 Myr), according to CK95, which strongly

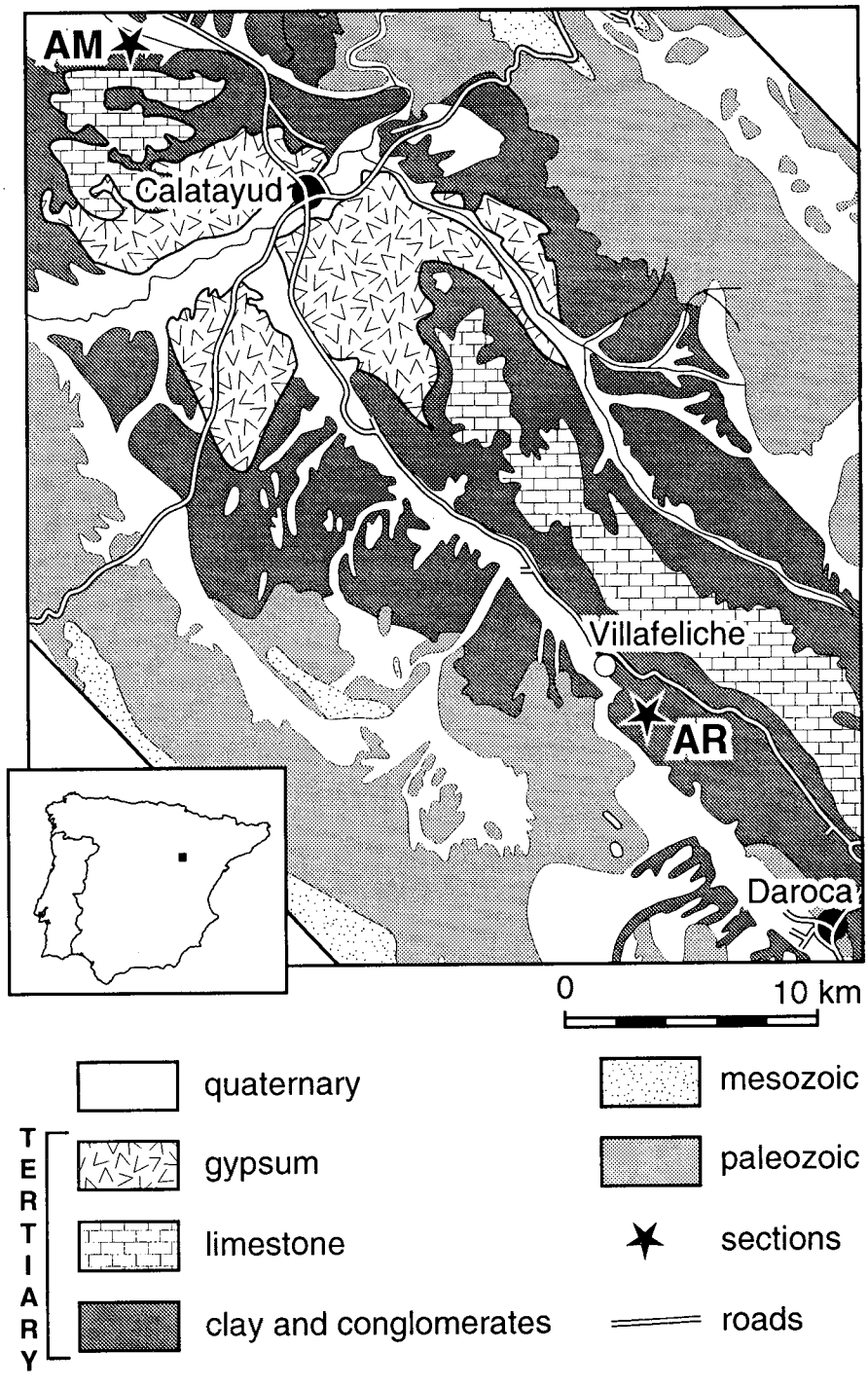

Figure 1. Location of the Armantes (AM) section in the Daroca-Calatayud graben. The Aragon section (AR) is time-equivalent with the Armantes section and has a very detailed biostratigraphic record (see Krijgsman et al., 1994b). Note that the depocenter of the Tertiary basin around Calatayud is characterised by gypsum deposits, while towards the margins lacustrine carbonates silts and coarse clastics occur.

Figura 1. Situación de la sucesión de Armantes (AM) en la cuenca de Calatayud-Daroca. La sucesión de Aragón (AR) es cronológicamente equivalente a la sucesión de Armantes y presenta un registro bioestratigráfico muy detallado (Krijgsman et al., 1994b). El depocentro de la cuenca terciaria en la región de Calatayud está caracterizado por depósitos de yeso, que hacia los márgenes pasan a carbonatos lacustres, lutitas y sedimentos terrígenos gruesos.

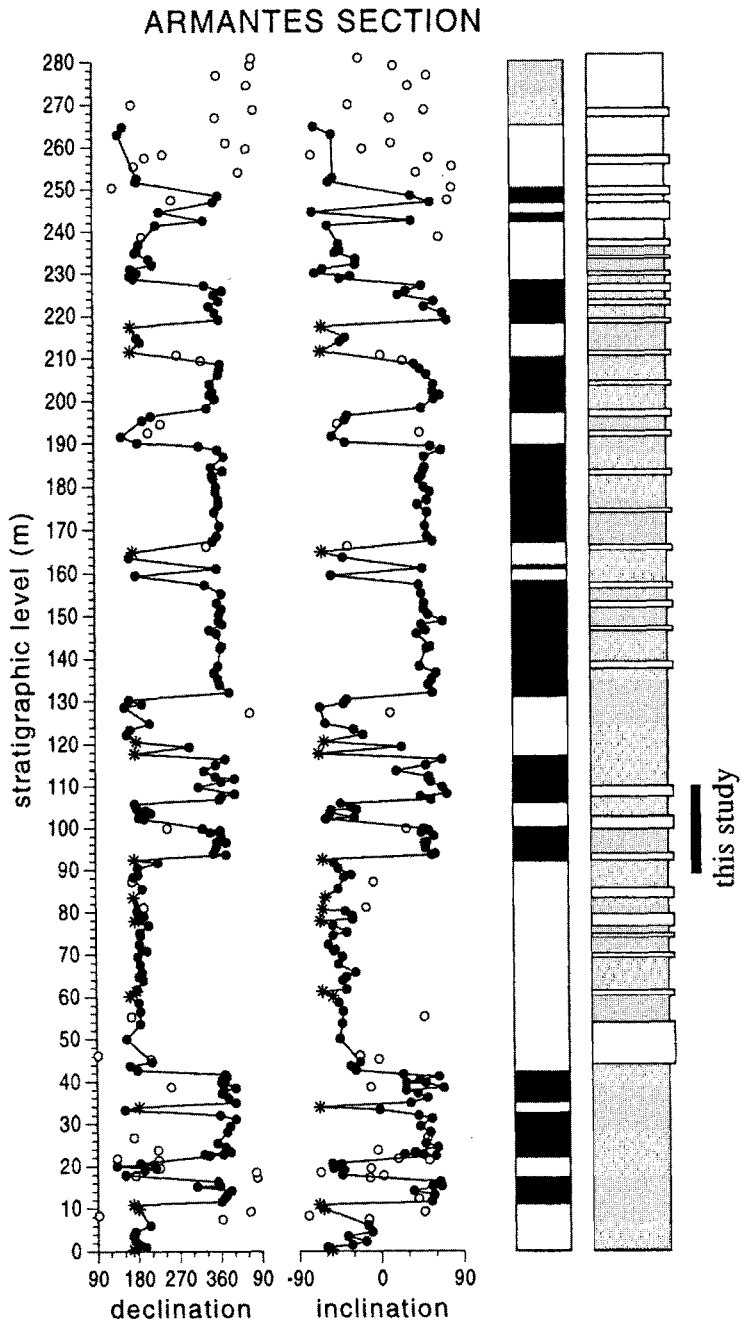

Figure 2. Magnetostratigraphy and lithology of the Armantes section (after Krijgsman et al., 1994b). Solid dots represent reliable directions, circles represent low intensity samples which are difficult to interpret. Asterisks represent directions obtained by applying the great circle method. In the polarity column, black (white) denotes normal (reversed) polarity zones; the shaded interval in the top of the section denotes a zone of uncertain polarity.The lithology column displays variations of red coloured silts and conglomerates (shaded) and pink/white coloured limestones (white).

Figura 2. Sucesión litoestratigráfica y magnetoestratigráfica de Armantes según Krijgsman et al., 1994b. Los puntos negros representan direcciones fiables. los círculos representan direcciones de muestras con baja intensidad y difícilmente interpretables. Los asteriscos representan direcciones obtenidas a partir del método de círculos máximos. En la sucesión de polaridad magnética el negro (blanco) representa polaridad normal (inversa). El tramo sombreado a techo de la sucesión representa una zona de polaridad incierta. La sucesión litológica muestra una alternancia de niveles lutíticos rojos con conglomerados (sombreado) y niveles calizos blancos y rosados (en blanco).

suggests that it is related to the ~100 kyr eccentricity cycle of the Earth's orbit (Krijgsman et al. 1994b).

Considering published data on red beds, there has always been serious doubt on their value for magnetostratigraphic and paleomagnetic studies. The remanence of red beds resides for a large part in hematite grains which are often considered to be of chemical and thus post-depositional origin (Walker et al., 1981). However, as shown by Van den Ende (1977), hematite grains in red beds can also be of synsedimentary origin and contain a depositional remanent magnetisation (DRM) In that case, they are capable of displaying paleosecular variations. If hematite carries a chemical remanent magnetisation (CRM), there are several possibilities for the origin of the hematite and its remanent magnetisation. Hematite can be created during early diagenesis or even recently by weathering (Roy and Park, 1972; Walker et al., 1981; Channell et al., 1982). Hematite can also be introduced into sediments by ground-water currents (Langereis and Dekkers 1992). Hence, CRM acquisition of hematite can be considered a long-term process, so that the CRM may comprise different paleomagnetic components and thus may not always be accurately dated. If, however, the hematite and its CRM has been created within a relatively short time interval, then the secondary paleomagnetic directions can be interpreted as delayed primary signals. Previous rock magnetic results from the Armantes section show that the natural remanent magnetisation (NRM) is defined by two components; hematite and magnetite (Dijksman, 1977; Krijgsman et al., 1994b). Throughout the section, there are variations in the relative amount of these two components which, in addition, are known to show a possible delay in acquisition (Dijksman, 1977).

To test the hypothesis of an astronomical origin of the distinct rhythmic bedding in the Armantes section, and to study the possible relation between the cyclic lithology variations and the acquisition of the NRM in these sediments, we sampled in detail a short stratigraphic interval. This interval contains three indurated limestone beds, which we infer to reflect the influence of the 100-kyr eccentricity cycle, and nine less distinct indurated beds in between.

THE ARMANTES SECTION

Geological setting and sampling

The Calatayud-Daroca basin is located in the Iberian Range, between the western and eastern Iberian Chains. The mountains adjacent to the basin consist of folded and faulted Paleozoic and Mesozoic rocks. Between Calatayud and Daroca, the basin is bordered by steeply dipping NW-SE trending normal faults with a dip towards the basin. Sediments in this area consist of conglomerates (along the borders of the basin), sands, silts, clays, and in the central part also lacustrine limestones and gypsum. The large body of evaporites (mainly gypsum) and limestones near the city of Calatayud, suggests that a lake existed in the deepest part of the graben, while red silts and intercalated white/pink limestones were deposited on the floodplain around the lake.

The Armantes section, approximately 12 km northwest of the city of Calatayud (Fig. 1), was first studied by De Bruijn (1965) for paleontological purposes and later by Dijksman (1977) and Krijgsman et al. (1994b), who showed that the sediments have paleomagnetic properties suitable for magnetostratigraphy. Correlation of the magnetic polarity sequence to CK95 (Cande and Kent, 1995) showed that a continuous succession from 17 to 12.5 Ma is present (Fig. 2; Krijgsman et al. 1994b). The Armantes section predominantly consists of a regular alternation of red silts and pink/white limestones. The nearly complete absence of primary sedimentary structures indicates that pedoturbation (desiccation, burrowing, rooting, paleosol development) has been intensive. Clear sedimentary structures were only found locally in rapidly deposited coarse-grained channel fills higher in the sequence, some 5 m above the top of the interval discussed here. The limestones are interpreted as "caliche horizons" and palustrine/lacustrine carbonates. The observed alternation is remarkably continuous both laterally and vertically. Throughout the section 27 indurated limestone beds have been recognised. For a detailed sampling, we selected the interval between limestone beds 7-9 (Fig. 2) because it is continuously exposed and accessible, because a smaller-scale cyclicity is well-developed, and because it contains three magnetic reversals. Correlation to CK95 shows that it concerns the chron interval C5Bn.1n-C5Br with an age from 15.2 to 14.9 Ma.

Over a stratigraphic distance of 22 m we sampled at 119 levels which corresponds to an average resolution of 18 cm (2.5 kyr). At each level we aimed to drill two oriented standard paleomagnetic cores. Some levels were impossible to drill and unoriented handsamples were taken.

Initial susceptibility and anisotropy

The initial susceptibility (χ_{in}) and the magnetic anisotropy of the samples were measured on a Kap-

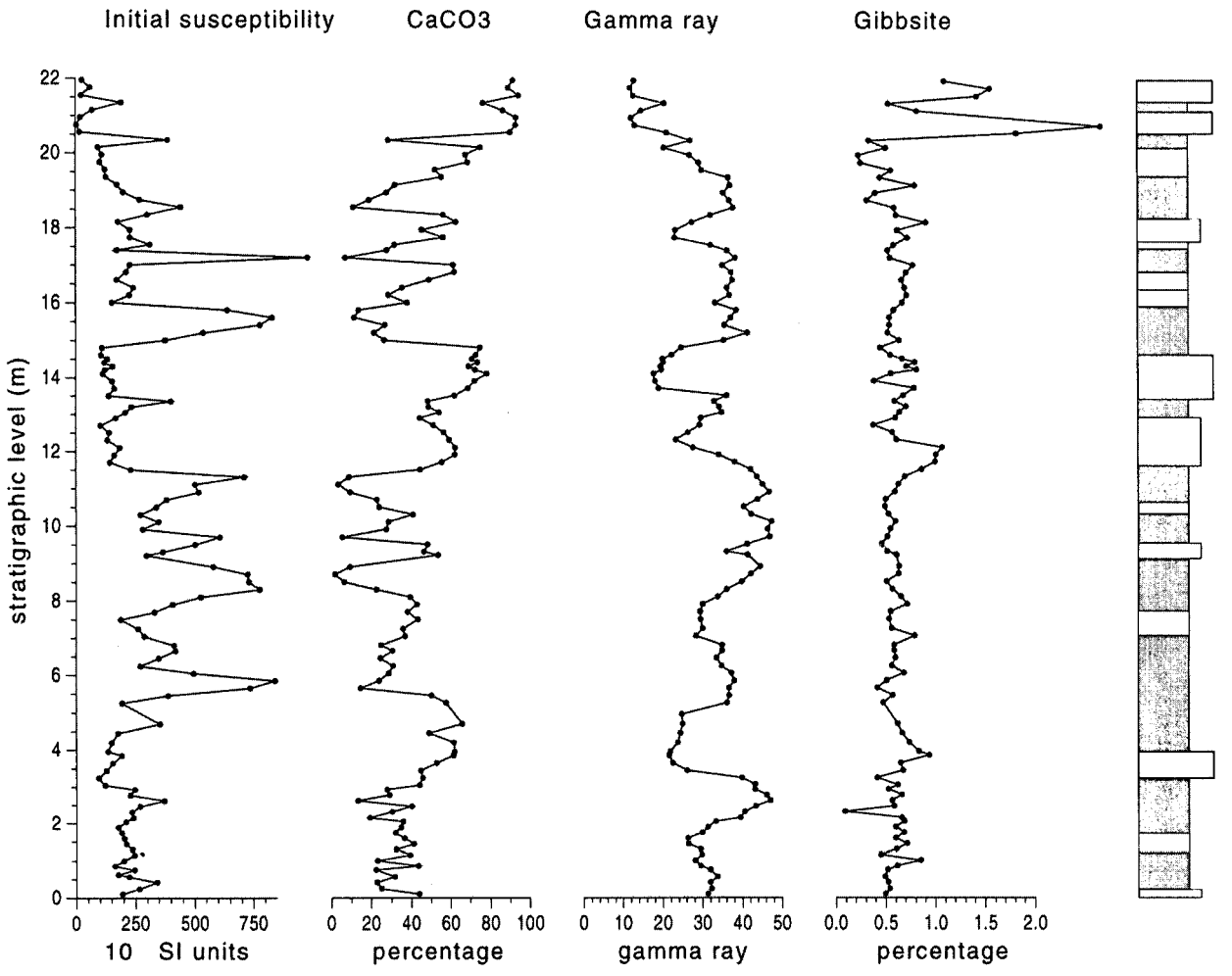

Figure 3. Initial susceptibility, carbonate concentration, gamma ray and gibbsite of the studied interval of the Armantes section. The lithology column displays red silts (dark shaded) smaller-scale bedding (shaded) and pink/white limestones (white). All records show a clear relation with the lithology. In the silts, the initial susceptibility and the gamma ray is relatively high while the carbonate concentration is low. Note also the increasing trend in the carbonate concentration from bottom to top.

Figura 3. Susceptibilidad inicial, concentración de carbonato, rayos gamma y contenido en gibbsita a lo largo del tramo estudiado en la sucesión de Armantes. La sucesión litológica está representada por limos rojos (sombreado oscuro), niveles finamente estratificados (sombreado) y calizas blancas/rosadas (blanco). Todos los parámentros representados presentan una visible correlación con la litología. En los limos los valores de la susceptibilidad inicial y rayos gamma son relativamente altos, mientras que la concentración de carbonato es baja. Nótese también la tendencia general hacia un aumento en la concentración de carbonato de base a techo.

pabridge KLY-2. The χ_{in} is strongly dependent on the concentration of paramagnetic (clay) minerals, on the concentration of ferrimagnetic minerals, and on the grain size and the type of magnetic mineral. The results from the Armantes section show that a clear relation exist between cin and lithology. The red silt beds show a relatively high χ_{in}, up to a maximum of 950 x 10^{-6} (SI), while the white limestone beds show a lower cin of 200-300 x 10^{-6}. The smaller-scale light red intercalations show intermittent values (Fig. 3).

For the oriented samples, the magnetic anisotropy of the initial susceptibility was determined. The anisotropy is generally 1-2 %, the minimum χ_{in}axes are on average vertical, the intermediate and maximum axes are randomly oriented in a horizontal plane (Fig. 4). The anisotropy can be caused by a large contribution of paramagnetic clay minerals or by hematite, which has a high intrinsic anisotropy. The Flinn diagram shows that the fabric causing the anisotropy is entirely foliated (oblate), and has no superimposed lineation. This strong oblateness of the fab-

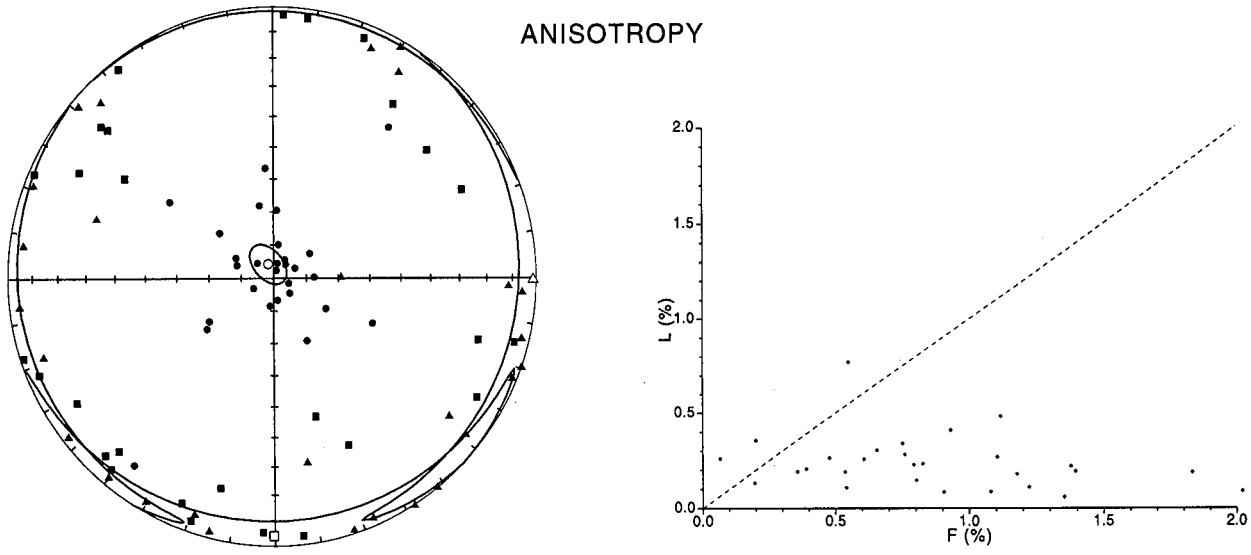

Figure 4. Anisotropy of the initial susceptibility. (A) Principal axes of the anisotropy; dots denote minimum axis, triangles intermediate axis and squares maximum axis. Open symbols denote the mean direction of the principal axes. (B) Flinn diagram; L = lineation, F = foliation. The magnetic fabric is oblate which indicates that deposition has taken place on a horizontal plane in a quiet sedimentary environment without any currents.

Figura 4. Anisotropía de la susceptibilidad inicial. (A) Ejes principales de anisotropía, círculos representan los ejes mínimos, triángulos los ejes intemedios y cuadrados los ejes máximos. Símbolos en blanco representan las direcciones medias de los ejes principales de anisotropía. (B) Diagrama de Flinn: L, lineación; F, foliación. La fábrica magnética es lenticular, que sugiere un depósito sobre una superficie horizontal en un ambiente sedimentario tranquilo sin fuertes corrientes.

ric indicates that deposition has taken place on a horizontal surface in a quiet sedimentary environment.

Carbonate concentration and clay minerals

The carbonate concentration was determined in the laboratory by measuring the quantity of hydrochloric acid (1N HCl) needed to dissolve the carbonate. After dissolution of the carbonate, the clay minerals were analysed using thermogravimetric analysis (TGA). For some levels X-ray diffraction analyses were made. The carbonate concentration of the samples displays a strong correlation with the observed lithology and erosion resistance in the field. It ranges between approximately 5-40 % for the red silt beds and 60-95 % for the pink/white limestone beds. The smaller-scale rhythmites have carbonate concentrations between 40 and 60 %. A general increase of carbonate content is observed from the bottom to the top of the section, and accompanies an increase of thickness of erosion-resistent beds (Fig. 3).

The X-ray diffraction analysis shows that the clay minerals predominantly consist of illite and to a lesser extent of kaolinite. Few samples possibly contain small amounts of chlorite and smectite. A TGA peak, observed around 300°C, is ascribed to gibbsite. X-ray diffraction indeed reveals a weak and scattered signal around 4.85 Å. Gibbsite is an aluminum-hydroxide which is produced in soils under humid and warm conditions (Füchtbauer, 1988). Aluminum can be dissolved in fluids with a PH of 7-8.5, a common range for water associated with carbonate deposits (Hay and Wiggins, 1980). The concentration of gibbsite displays a relation with the lithology, relatively high values occuring just beneath and within the bottom part of the thick limestone beds (Fig. 3). This suggests that these limestone beds were deposited under humid and warm conditions.

Gamma ray

The gamma ray signal at each level was measured in the field with a WG 135 differential Gamma Spectrometer. The gamma-ray record generally reflects the amount of clay minerals in the sediment. As expected, it reveals relatively high values for the clayey silt beds and low val-

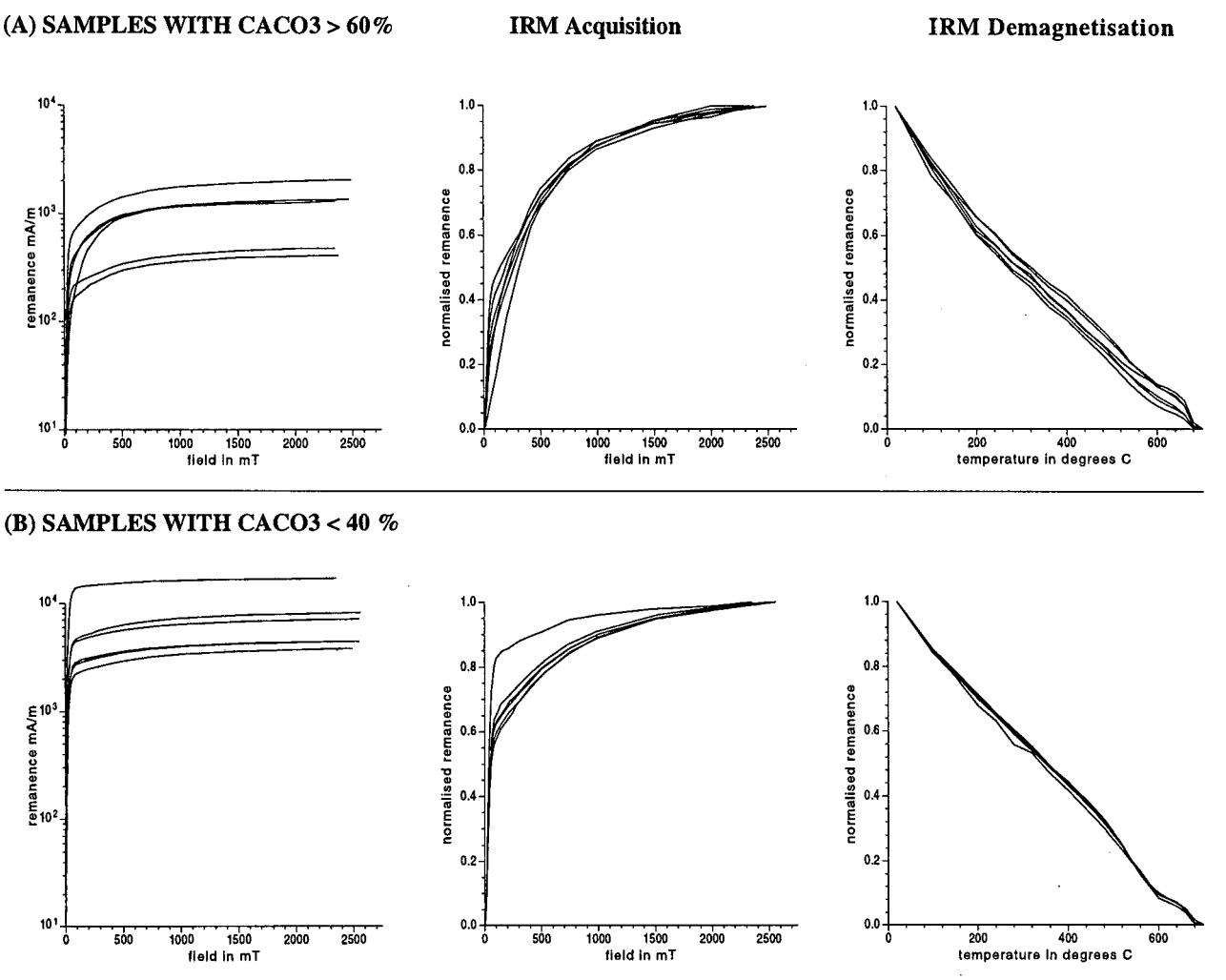

Figure 5. Examples of IRM acquisition (absolute and normalised values) of samples from limestones with carbonate concentration > 60% and from silts with carbonate concentration < 40%. The initial steep rise (< 200 mT) points to magnetite, the gradual increase at high fields (> 200 mT) suggests the additional presence of hematite. Stepwise thermal demagnetisation of the normalised IRM also shows the presence of both magnetite or partially oxidised magnetite (maghemite) (580-600 °C) and hematite (680 °C), particularly in the silts.

Figura 5. Ejemplos de adquisición de magnetización remanente isotérmica (valores absolutos y normalizados) de muestras de calizas con concentración de carbonato superior a 60% y limos con concentración de carbonato menor que 40%. La rápida subida inicial (<200 mT) indica la presencia de magnetita, mientras que el crecimiento gradual para campos mayores que 200 mT sugiere la presencia adicional de hematites. La desmagnetización térmica progresiva de la magnetización remanente isotérmica también muestra la presencia de magnetita, o magnetita parcialmente oxidada (maghemita) a 580-600°C y hematites a 680°C, especialmente en las muestras de lutitas.

ues for the limestone beds, thus showing a clear negative correlation with the carbonate concentration (Fig. 3). The gamma-ray record shows a much smoother function than the carbonate and χ_{in} records. This is caused by scattering of gamma ray radiation from adjacent beds. A decreasing trend from bottom to top of the sampled interval is in agreement with the gradually increasing carbonate content and the decreasing susceptibility.

PALEOMAGNETIC RESULTS

Methods

We performed some rock magnetic experiments to investigate the influence of the type of lithology on the NRM acquisition. An isothermal remanent magnetisation (IRM) was acquired on a PM4 pulse magnetiser up to

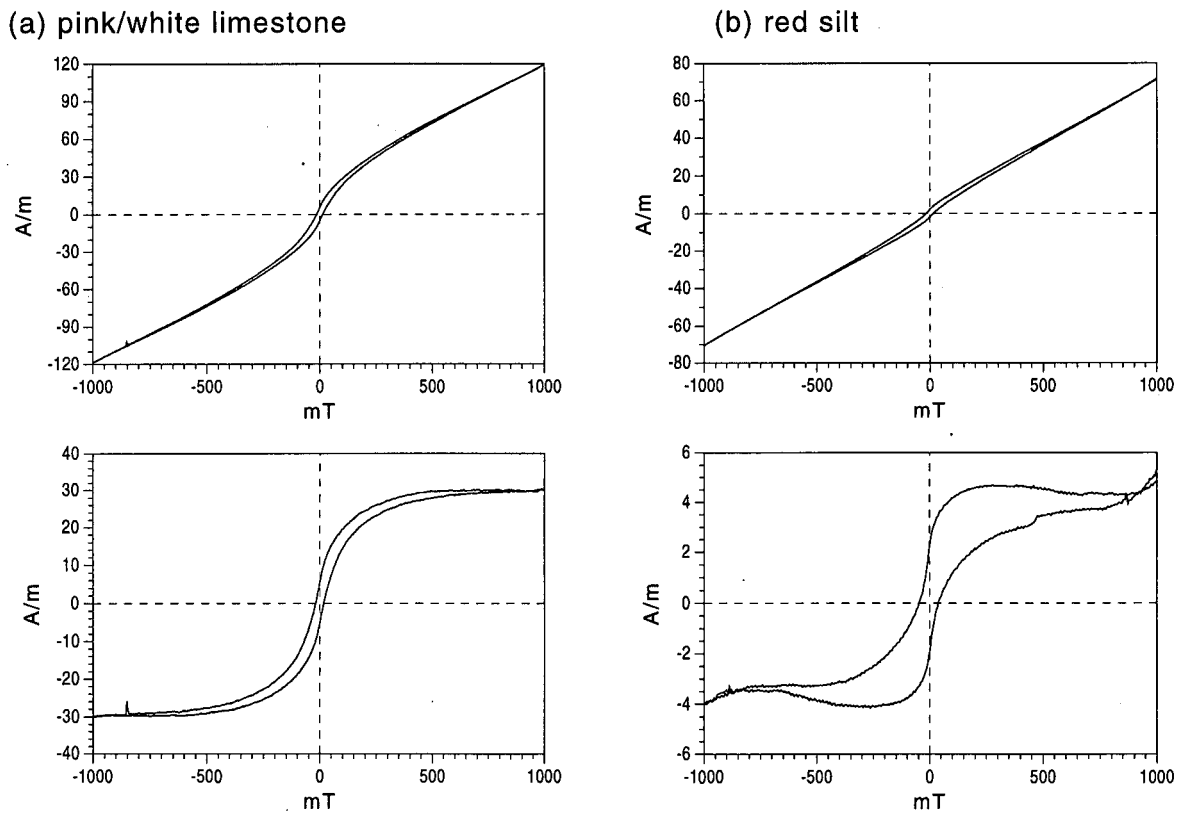

Figure 6. Hysteresis loop and corrected (for paramagnetic contribution) hysteresis loop of a selected sample from the limestones and from the silts. The strong increase at low magnetic fields points to magnetite, the fact that saturation is not achieved in the highest possible field of 1 Tesla suggests the presence of hematite.

Figura 6. Ciclos de histéresis normales y corregidos por la contribución paramagnétcia de muestras seleccionadas de calizas y lutitas. El fuerte incremento para valores de campo bajos indica la presencia de magnetita, mientras que la no saturación para campos de 1 Tesla sugiere la presencia también de hematites.

maximum fields of 2400 mT and was measured on a JR5 spinner magnetometer. Hysteresis loops and (remanent) coercive force values (Hc, Hcr) of all samples were measured on a alternating gradient force magnetometer model 2900. Both the NRM and the IRM were thermally demagnetised in a laboratory-built shielded furnace, with small temperature increments of 30-50°C, up to a maximum of 700°C. The NRM was measured on a 2G Enterprises horizontal cryogenic magnetometer equipped with DC SQUIDS. Susceptibility was measured after each temperature step on a Kappabridge KLY-2.

IRM acquisition and subsequent demagnetisation

IRM acquisition curves were determined for all drilled samples. They indicate the presence of two different components (Fig. 5). A steep rise between 0 and 100-200 mT suggests the presence of a low-coercivity mineral like magnetite or maghemite. At higher fields, the IRM acquisition curves increase gradually. Even at the highest field values of 2400 mT, saturation is generally not reached. This indicates the presence of a high-coercivity mineral like hematite and/or goethite. The relative part of the IRM which is caused by the high-coercivity mineral was estimated by extrapolation to the relative intensity axis, from the point where the low coercivity mineral is saturated. For the silts it shows that the IRM mainly (60-85%) consists of the low-coercivity component. For the limestones the contribution of the low-coercivity minerals to the IRM is relatively low (0-20 %), and the IRM is dominated by the high-coercivity mineral.

The IRM demagnetisation curves confirm the presence of two different components. An unblocking tem-

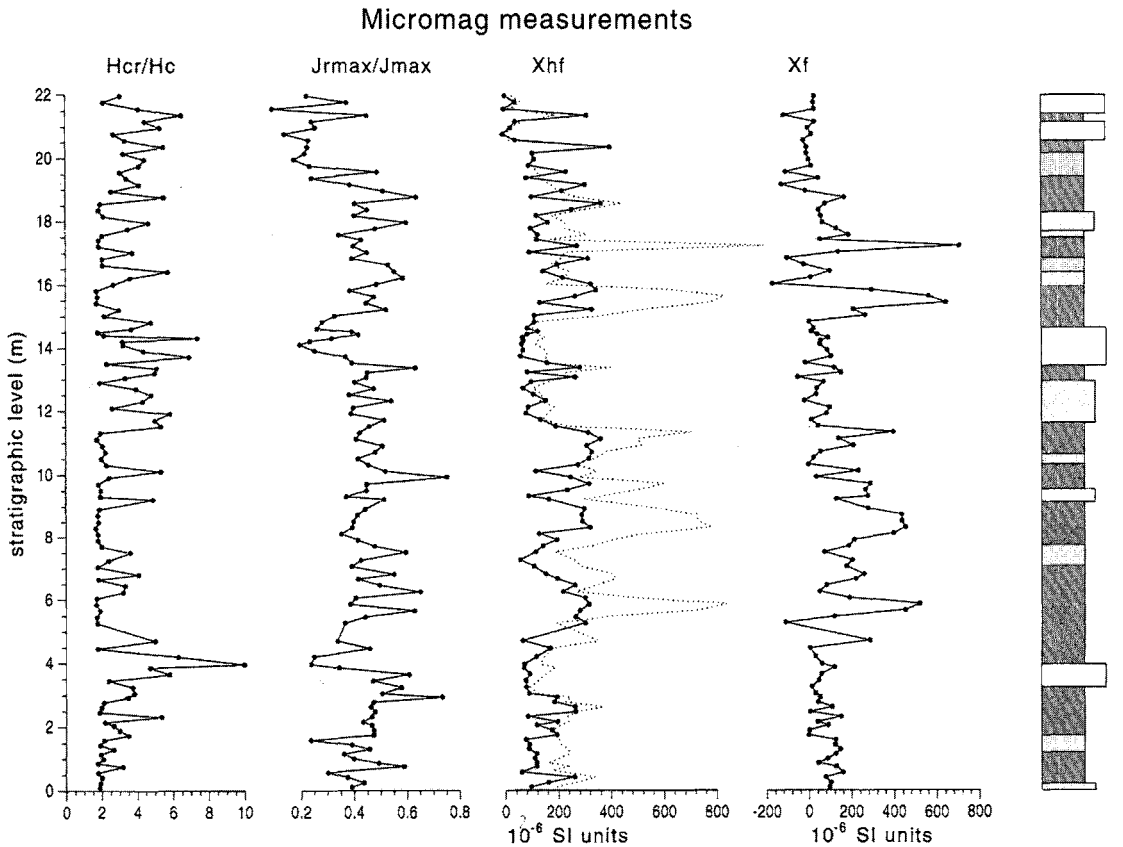

Figure 7. Micromag measurements displaying the coercive force ratio H_{cr}/H_c, the magnetisation ratio J_{rmax}/J_{max}, the paramagnetic susceptibility χ_{hf} and the ferrimagnetic susceptibility χ_f (= χ_{in}- χ_{hf}) versus stratigraphic level. H_{cr}/H_c is relatively high, while in the limestones J_{rmax}/J_{max}, χ_{hf} and χ_f are relatively low. Dotted line denotes the initial susceptibility χ_{in}.

Figura 7.Variación de diferentes parámetros magnéticos en función de la posición estratigráfica. H_{cr}/H_c: Tasa de fuerza coercitiva; J_{rmax}/J_{max},: Tasa de magnetización; chf: Susceptibilidad paramagnética; cf (= χ_{in}- χ_{hf}): Susceptibilidad ferrimagnética. H_{cr}/H_c es relativamente alto, mientras que en las calizas J_{rmax}/J_{max}, χhf y χf son relativamente bajos. La línea punteada representa la susceptibilidad inicial χ_{in}.

perature of 580-600°C, which is clearly visible in the curves of the silt beds, is somewhat high for magnetite and could indicate the presence of partially oxidised magnetite (maghemite) (Fig. 5). All curves show an additional unblocking temperature of 680°C which indicates the presence of hematite as the high-coercivity mineral. The IRM demagnetisation curves show no significant decrease below 100°C which suggests that the contribution of goethite is negligible.

Coercive forces

The hysteresis loops display the contribution of the paramagnetic clay minerals to the total magnetisation. After correcting for the paramagnetic part, usually two different types of loops can be observed (Fig. 6). Both hysteresis loops show that the sample consists of magnetite, characterised by the strong increase at low magnetic fields, and of hematite, considering the fact that the hysteresis loops are not saturated at high magnetic fields. However, the shape of both hysteresis loops is very different. The "wasp waisted" shape of the corrected silt-bed hysteresis loop may have been caused by the presence of viscous (or superparamagnetic) magnetic minerals. It is more likely, however, that the "wasp-waisting" in this case is caused by a mixture of high and low coercivity minerals (Tauxe et al., 1995).

The coercive force (H_c) and remanent coercive force (H_{cr}) values clearly display the presence of both magnetite and hematite. For samples containing relatively

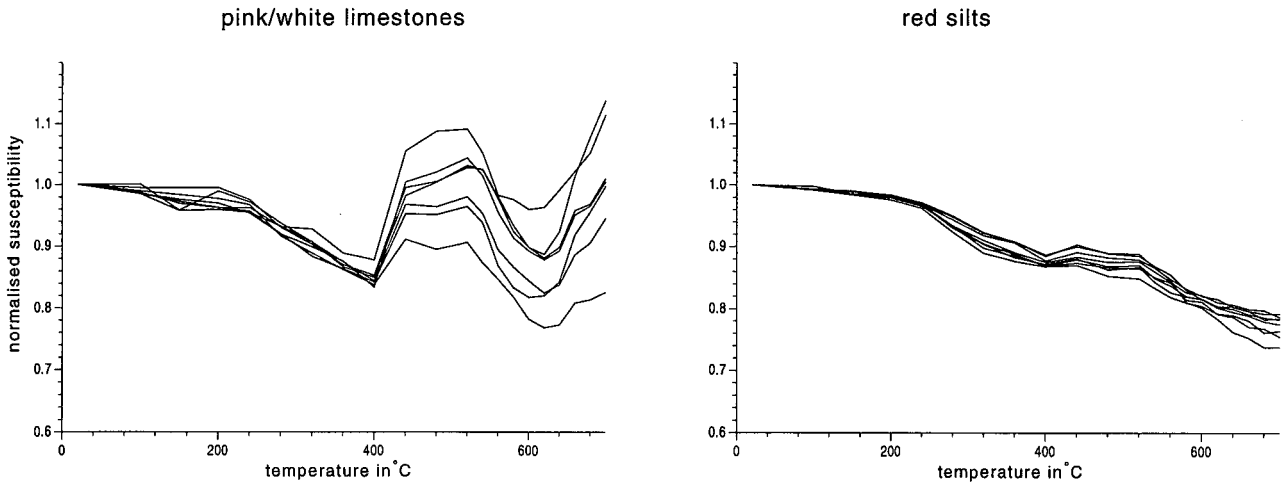

Figure 8. Bulk susceptibility during thermal demagnetisation of the IRM. (A) examples from the limestone interval between 13.5-14.5 m (B) examples from the silty interval between 7.0-9.0 m. The increase in susceptibility between temperatures of 400°-500 °C might be caused by a production of more magnetic impurity in small-hematite grains. The increase in susceptibility at temperatures higher than 600 °C is possibly related to the presence of an Fe-bearing clay mineral.

Figura 8. Variación de la susceptibilidad magnética durante la desmagnetización térmica de la magnetización remanente isotérmica. (A) ejemplos del intervalo de calizas entre 13.5 y 14.5 m. (B) ejemplos del intervalo lutítico entre 7.0 y 9.0 m. El aumento de susceptibilidad entre 400° y 500 °C puede estar originado por la formación de partículas magnéticas de hematite de grano muy fino. El aumento de susceptibilidad a temperaturas superiores a 600°C puede estar relacionado con la presencia de arcillas con alto contenido en hierro.

much magnetite, the H_{cr} values are approximately 30 mT, while for the samples containing mostly hematite, the H_{cr} ranges between 100 mT and 300 mT. The coercive force ratio (H_{cr}/H_c) shows a strong relation with the lithology (Fig. 8). H_{cr}/H_c displays high values for the thick limestone beds and lower values for the silts. These observations imply that hematite is dominantly present in the limestones. Also higher ratios are observed around the smaller indurated beds suggesting that these beds contain also a higher concentration of hematite. The ratio between the maximum remanent magnetisation (J_{rmax}) and the maximum magnetisation (J_{max}) displays the inverse correlation with the lithology (Fig. 7). Low magnetisation ratios (J_{rmax}/J_{max}) in the limestones indicate the presence of relatively large concentrations of hematite. J_{rmax}/J_{max} shows also a strong relation with the presence of viscous magnetite minerals; in the silt samples, which contain viscous magnetic minerals, J_{rmax}/J_{max} is generally higher.

Susceptibility

The initial susceptibility (χ_{in}) consists of a ferrimagnetic part (χ_f), caused by magnetic minerals, a paramagnetic part, the so-called high-field susceptibility (χ_{hf}), caused by paramagnetic clay minerals, and a diamagnetic part cdia, caused by carbonates and quartz. The chf was determined from the slope of the hysteresis loops at the highest available fields of 1.4 Tesla. Hence, the cf was determined by substracting the chf from the χ_{in} (Fig. 7). Some samples, however, show a negative χ_f, which is physically impossible. These negative values result from the fact that the determined χ_{hf} is too high, which must be caused by a very high concentration of hematite and the fact that hematite is often not saturated at the highest fields (Fig. 5). Inhomogeneity in the sediment and the very small sample size for the Micromag may also result in too high χ_{hf} values.

During thermal demagnetisation of the IRM we also measured the bulk susceptibility after each temperature increment. Both the limestones and silts show a decrease of χ_{in} above 200°C (Fig. 8). An increase in χ_{in} is observed at temperatures above 400°C, reaching its peak value at 510°C, while a subsequent decrease follows till 600°C. Dekkers and Linssen (1989) suggest that the increasing susceptibility in fine-grained hematite above 400°C can be caused by production of more ferrimagnetic impurity, which was also noted by Dunlop (1971). This impurity in hematite can be maghemite which would disappear by in-

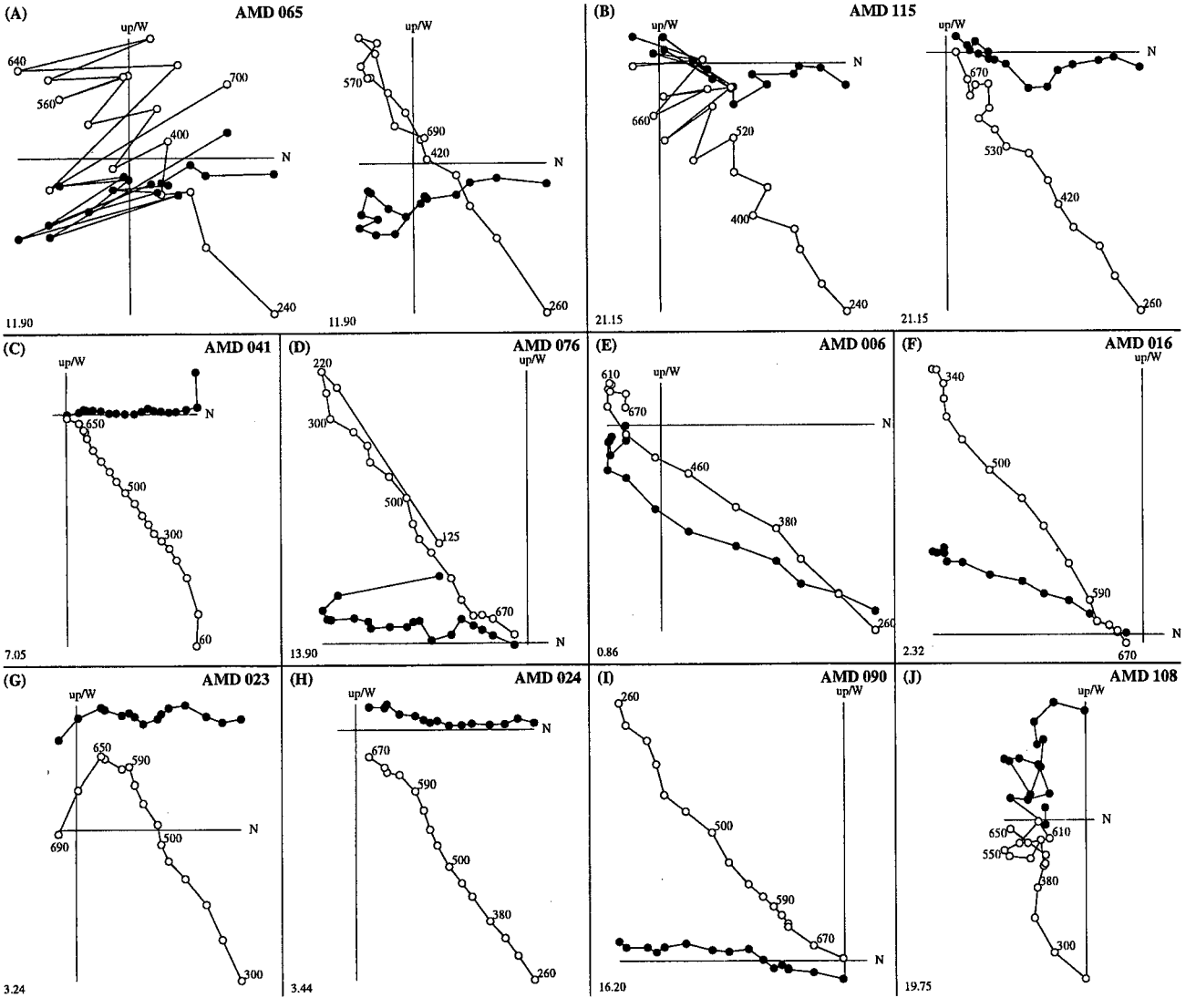

Figure 9. Thermal demagnetisation diagrams of selected samples from the Armantes section. Closed (open) circles denote the projection on the horizontal (vertical) plane; values are temperature steps in °C; stratigraphic levels are in the lower left corner. (A) and (B) are examples showing the effects of applying a two-point running average on the original data which are suffering from a viscous component that is related to a small residual field in the furnace. (C) shows the randomly oriented laboratory component at room temperature. (D) shows the secondary present-day field component which is generally removed at 240°C. (E)-(I) are characteristic samples showing both a MT (magnetite) and a HT (hematite) component. Note that these two components do not always have the same polarity. An example from the upper part of the section in which the intensities for both the MT as HT component are relatively low is shown in (J).

Figura 9. Diagramas de desmagnetización térmica de muestras representativas de la sucesión de Armantes. Círculos negros (blancos) representan la proyección sobre el plano horizontal (vertical) de los diferentes pasos de temperatura en grados Celsius; el nivel estratigráfico de cada muestra indicado en la esquina inferior izquierda. (A) y (B) son ejemplos en los que se ha promediado el dato original entre pasos consecutivos para atenuar el efecto de la componente viscosa relacionada con el pequeño campo residual presente en el horno. (C) representa el campo magnético del laboratorio a temperatura ambiente. (D) muestra la componente secundaria de campo actual que se desbloquea a 240 °C. (E)-(I) representa muestras características con componentes MT (magnetita) y HT (hematites). Nótese que los dos componentes no presentan siempre la misma polaridad. Un ejemplo de la parte superior de la sucesión donde las intensidades de MT y HT son relativamente bajas se muestra en (J).

version to hematite at temperatures of approximately 600°C. When natural goethite is converted into hematite, also trace amounts of magnetite can be produced (Dekkers, 1988). The relative increase in χ_{in} during thermal demagnetisation is generally higher in the limestones than in the silts, probably because the relative contribution of hematite is larger in the limestones. Furthermore, it might have been emphasised by the normalisation of cin on the basis of its initial value, which is much smaller for the limestones. The high-carbonate samples show again an increase of cin above 600°C (Fig. 8). This increase in cin is not well-understood.

NRM demagnetisation

The determination of reliable directions from the thermal demagnetisation diagrams was strongly hampered by a large disturbing magnetisation component, probably caused by a small residual field in the furnace (Fig. 9a,b). As a standard procedure, the samples are placed in an opposite position in the furnace at every subsequent temperature step. To obtain more reliable directions we averaged the direction and intensity afterwards by calculating a two-point running average. The thermal demagnetisation diagrams of these averaged directions clearly show that the NRM consists of several components (Fig. 9c-j). A small component is usually removed at temperatures of 100°C; it is randomly directed, and thus has a viscous origin rather than being due to goethite. A secondary component is removed at temperatures of 240°C. This component has an approximately present-day field direction and is of subrecent origin. After these components are removed, two other components could be observed. One relatively low temperature (LT) component is generally removed at temperatures below 600°C, suggesting magnetite, and another high temperature (HT) component at temperatures of 680°C, indicating hematite. For some samples, the total remanence is not entirely removed at the highest temperatures. Apparantly, the two-step averaging procedure does not entirely remove the disturbing magnetisation component induced by the very low magnetic residual field in the furnace.

DISCUSSION

Lithological cycles

Calcretes and caliche are commonly interpreted to have formed in semiarid to arid, warm seasonally dry climates (Blodgett, 1988). Of course, the prerequisite for the formation of calcrete (caliche) is an adequate supply of (dissolved) calcium carbonate. The absence of channel and current structures in the studied part of the succession suggests that carbonate was supplied along with the ground water, which was fed from adjacent topographic highs through marginal alluvial fan deposits to the lower parts of the basin. Precipitation of the carbonate, as caliche nodules, calcretes and dispersedly through the sediment must have occurred during evaporation of the ground water in the topographically lower parts of the basin. Supply of carbonate as eolian dust may have played a role as well, but also in that case, (ground)water must have been present to allow vegetation (as observed from local root traces), and redistribution and concentration of carbonates. It is inferred that, during deposition of the studied interval, the basin, or the part of the basin in which the studied sequence was deposited, had an internal drainage most of the time. Only when water supply exceeds evaporation, external drainage will occur, and dissolved carbonates may be exported from the basin, either dissolved in ground water or as part of the surface runoff. The cyclic occurrence of carbonate-rich beds thus is interpreted to be the result of regular changes in the humidity.

NRM acquisition

A good paleomagnetic record in which polarity reversals can be accurately determined, is essential for the construction of an APTS. The rock magnetic results of the Armantes section clearly indicate that at least two components contribute to the NRM of these sediments and that the importance of each component depends on the type of lithology. IRM acquisition curves and hysteresis loops indicate that both a low-coercivity and a high-coercivity mineral are dominantly present in all samples. Relatively high blocking temperatures - between 680-700°C - of both the NRM and IRM, corresponding to levels with high Hcr values, indicate that hematite is the high-coercivity mineral. Blocking temperatures between 580-600°C, corresponding to levels with low H_{cr} values, suggest that magnetite or/and maghemite (partially oxidised magnetite) is the low-coercivity mineral. The existence of maghemite as ferrimagnetic impurity can explain the increases in cin at temperatures between 400-500°C during thermal demagnetisation.

Due to the difference in blocking temperature, the hematite component can be separated from the magnetite component after thermal demagnetisation. In the interpretation of the demagnetisation diagrams we distinguished two components; a LT component determined in the temperature range 400-600°C, characteris-

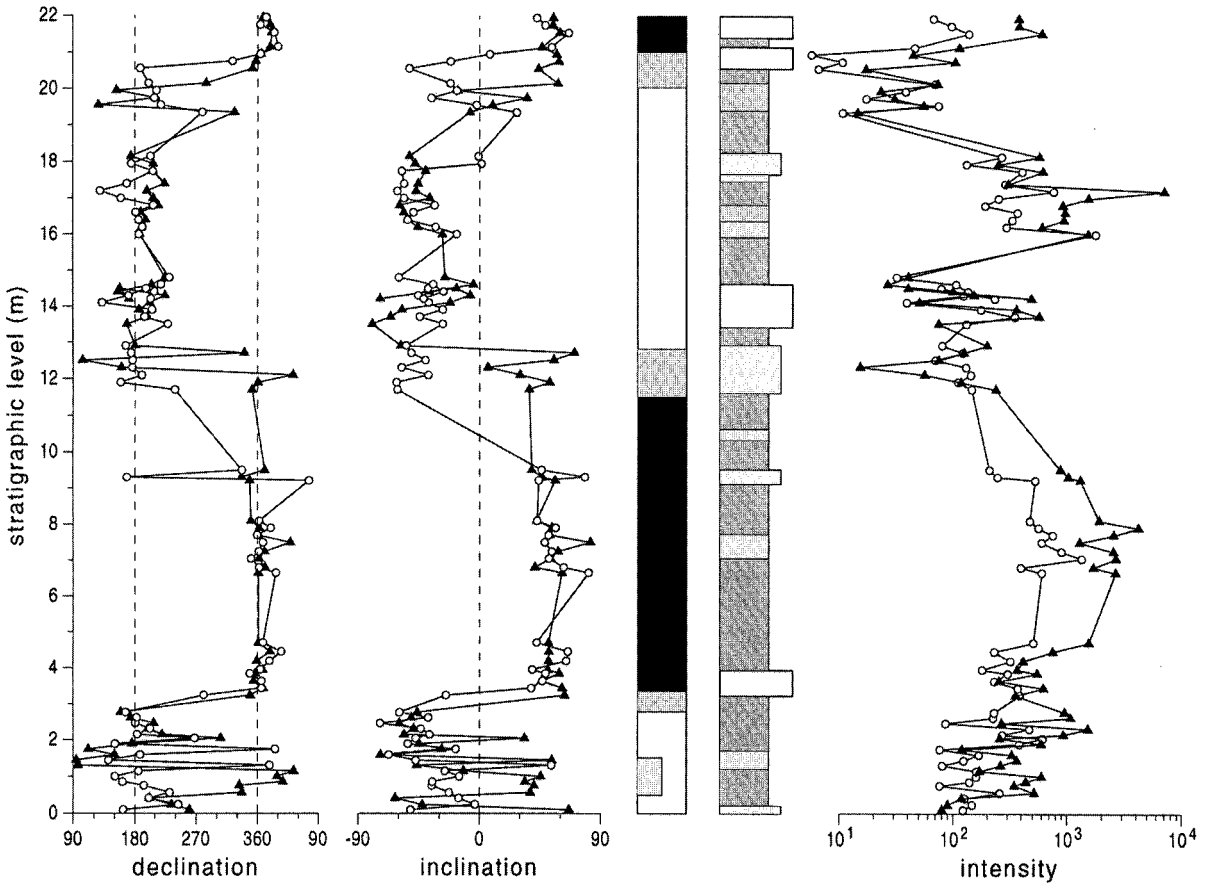

Figure 10. Magnetostratigraphy, lithology and the intensities for the three components of the detailed studied part of the Armantes section. Triangles represent directions of the MT (400-600 °C) component, related to magnetite and/or maghemite. Solid dots represent directions of the HT (600-700 °C) component, which is related to hematite. See also caption to figure 2.

Figura 10. Declinación, inclinación e intensidad de las componentes paleomagnéticas observadas en el tramo de la sucesión de Armantes analizado en el presente estudio. La componente de temperatura intermedia (400-600 °C), con triángulos, se atribuye a magnetita y/o maghemita. Los círculos representan la componente de alta temperatura (600-700 °C), que se atribuye a hematites. Ver también pie de figura 2.

tic for magnetite, and a HT component (600-700°C) characteristic for hematite. The LT and HT components both show reversed and normal polarities, suggesting a near primary origin, but they sometimes show opposite polarities at the same level or interval (Fig. 10). In the lowermost part (0-3 m) of the section, the HT component is predominantly reversed while the LT component shows normal polarities between 0.5-1.5 m (Fig. 10, 9e,f). These normal magnetic directions may be related to a cryptochron, although this was never recorded before at the corresponding age.

The lowermost polarity transition (3-3.5 m), from reversed to normal, appears to occur slightly "earlier" (i.e. lower in the stratigraphy) in the LT component than in the HT component (Fig. 9f-h). This lower transition in the LT component is also observed at the uppermost polarity transition (19-21 m), although the directions are less well determined because of a relatively lower intensity of both components (Fig. 10, 9j). However, the polarity transition from normal to reversed in the middle part of the section (12-13 m) suggests that there the reversal of the HT component is "earlier" than the LT component. Since all three polarity reversals occur near the thick (dominant hematite) limestone beds, the LT intensities are generally very low at the polarity transitions.

The results of this study show that a clear difference in magnetic composition exists between the white limestones and the red silts. In the limestones χ_{in} and

J_{rmax}/J_{max} are low, H_{cr}/H_c is high relative to that in the silts. IRM acquisition curves show that the relative contribution of hematite is 60-80 % in the limestones and only 20-40 % in the red silts. Hence, it is concluded that hematite is the dominant magnetic mineral in the limestones, whereas magnetite/maghemite is of major importance in the silts. Nevertheless, the absolute contribution of hematite to the IRM is higher in the silts, and thus the dominance of hematite in the limestones is controlled by a very low concentration of magnetite. The absolute concentration of hematite in the limestones is lower than in the silts.

The hematite, which gives these rocks their red colour, is probably authigenic, having grown from a precursor during early diagenesis. One argument that the hematite is authigenic rather than detrital comes from the limestones where spotty distributions of red colouration is such that hematite cannot be detrital in origin. A partial detrital origin for the hematite in the red silts can, however, not be excluded. Hematite pigment in red beds may be caused by a variety of diagenetic processes such as alteration of iron-magnesium silicates (Walker et al., 1981), the breakdown of iron-bearing clays (Walker and Honea, 1969) or dehydration of goethite (Channell et al., 1982). The hematite of the Armantes section probably also originates from oxidation of Fe-bearing precursors and/or precipitation upon oxidation of ground-water-dissolved reduced iron species, and thus carries a CRM. Precipitation of hematite from oxidising ground water was low in the silts due to a low evaporation rate. Consequently, also more magnetite grains are preserved which most likely generate the observed disturbing magnetic response in the silts. The process which controls the diagenetic growth of hematite thus seems to be related to the lithology and to the paleoclimate.

A possible mechanism for hematite growth in limestones, occurring during some time after deposition, was proposed by Channell et al. (1982). The CRM direction of the hematite grains depends on the ambient field at the time of growth through a critical volume and this direction does not change anymore during further growth. Channel et al. (1982) showed that the reversal of the largest hematite grains occurs earlier than the reversal of the detrital magnetite component, which indicates that some hematite grains may grow through their critical volume before the detrital magnetite component is fixed into the sediments. This mechanism may explain the "earlier" reversals of the magnetite component with respect to the hematite component in the lower and upper reversal.

CORRELATION TO THE ASTRONOMICAL CURVES

The earlier magnetostratigraphic and cyclostratigraphic study on the Armantes section showed that the distinct cyclic middle part of the Armantes section (54-235 m) covers approximately 3 Myr (Krijgsman et al, 1994b). In this part we counted 27 (large scale) cycles which results in an average periodicity of 111 kyr (Fig. 2), suggesting a relation with the eccentricity cycle of the Earth's orbit. To determine wether the cyclicity observed in the Armantes section is indeed related to the astronomical cycles, we applied spectral analysis on the astronomical solutions of La90 (Laskar, 1990) to determine which dominant frequencies are expected in the corresponding time interval. The frequency spectrum for the La90 eccentricity curve - using the CLEAN spectral analysis (Roberts et al., 1987) - shows that the corresponding interval (14.5-15.5 Ma) is determined by two equally strong peaks at 125 and 95 kyr, resulting in an average periodicity of 110 kyr (Fig. 11). This is in excellent agreement with the magnetostratigraphically estimated average periodicity of 111 kyr and confirms the suggestion that the generation of the thick limestone beds is related to the orbital eccentricity cycle. The smaller scale bedding (2-3 m) than is related to the precession cycle with main quasi-periodicities of 19, 23 and 25 kyr, according to La90. Indeed the carbonate, gamma-ray and susceptibility record show four smaller-scale peaks in between the thick limestone beds.

An important question is how to correlate the limestone beds to the eccentricity record. From a paleoclimatological point of view it is most logical to correlate the limestones to eccentricity maxima. During periods of maximum eccentricity the Earth is in perihelion during the northern hemisphere summer, summer temperatures are above average and winter temperatures below average. The orbital eccentricity defines the maximum possible insolation perturbations and precession defines the time of occurrence, i.e., when mid-winter and mid-summer equinoxes coincide with perihelion and aphelion (cf. Park and Oglesby, 1994). Increasing latitudinal temperature gradients during high eccentricity likely induce a greater depression activity, and hence an increased rainfall (cf. Valdes et al., 1995). A rise of the ground-water level resulting from the increased humidity thus would have allowed evaporation and the precipitation of carbonates as caliche nodules and carbonate crusts under marginal lacustrine conditions. From marine Pliocene sequences is has become clear that periods of increased humidity are connected with, among others, the monsoonal system which in turn results from orbitally forced variations in low latitude summer insola-

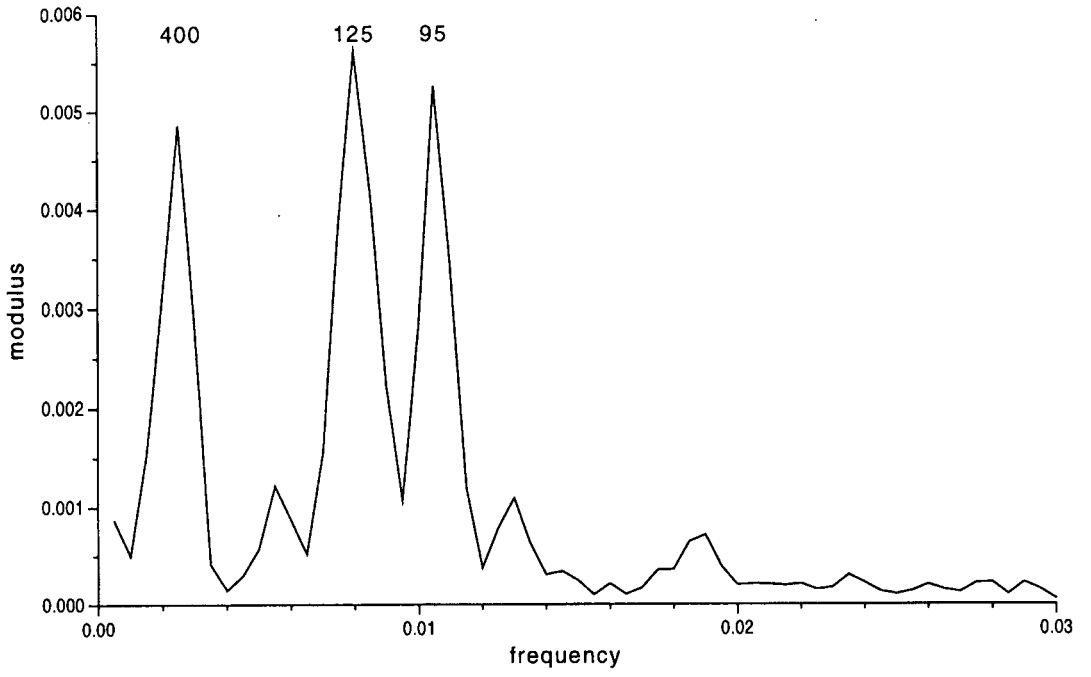

Figure 11. Frequency spectrum of the La90 solution for eccentricity. The amplitude of the spectral peaks corresponding to the 125 and 95 kyr periods are of similar magnitude. This corresponds to a mean period of approximately 110 kyr, as found in the Armantes record.

Figura 11. Distribución de frecuencias de la excentricidad de la solución La90 (Laskar, 1990). La amplitud de los picos correspondientes a los periodos de 125 y 95 kyr son de magnitud similar, y corresponden a un periodo medio de unos 110 kyr, como se observa en el tramo estudiado de la sucesión de Armantes.

tion, and correlate with periods of precession minimum (Rossignol-Strick, 1983; Rohling and Hilgen, 1991). Future research is needed to confirm the suggested relations between limestones and eccentricity.

To make a correlation to the astronomical curves, an independent age constraint is needed. In this study this is provided by the ages of the polarity reversals. The three reversals recorded in the section correspond to the chron boundaries C5Bn.2n(o) at 15.155 Ma, C5Bn.2n(y) at 15.034 Ma and C5Bn.1n(o) at 14.888 Ma (Krijgsman et al., 1994b). According to these ages of CK95, the interval between the youngest and oldest recorded reversal has a duration of 267 kyr. The same interval covers two large-scale eccentricity cycles which suggests only approximately 220 kyr (18% shorter). An explanation for this difference is an error in the ages of the calibration points in CK95. A magnetostratigraphic and cyclostratigraphic study on late Miocene sections on Crete (Krijgsman et al., 1994a) indeed showed that astronomically defined time spans are approximately 10 % shorter than expected in GPTS of CK92 (Cande and Kent, 1992).

The ages of the recorded reversals in our detailed studied part of the Armantes section are largely determined by the calibration point of 14.8 Ma in CK95, assigned to the younger end of chron C5Bn.1n(y). This is an average age based on radioisotopic age constraints on the correlative N9/N10 planktonic foraminifera zone boundary (Miller et al. 1985; Berggren et al., 1985), as estimated in Japan at 14.6 ± 0.04 Ma (Tsuchi et al., 1981) and in Martinique at 15.0 ± 0.3 Ma (Andreieff et al., 1976). However, Baksi (1993) presented a time scale, based on ages derived from $^{40}Ar/^{39}Ar$ incremental-heating of whole rock basalts, which suggests that chron C5Bn.1n is approximately 1 Myr older than indicated by CK95. Berggren et al. (1995) conclude that the Baksi (1993) time scale suffers from ambiguous correlations of isolated magnetic reversals to the GPTS. Astronomical ages for polarity reversals up to 9.5 Ma (Hilgen et al., 1995) are only slightly (50 kyr) older than in CK95 suggesting that the average age of 14.8 Ma of CK95 is probably a better estimate than the ages of Baksi (1993) but that a slightly older age can not be totally excluded.

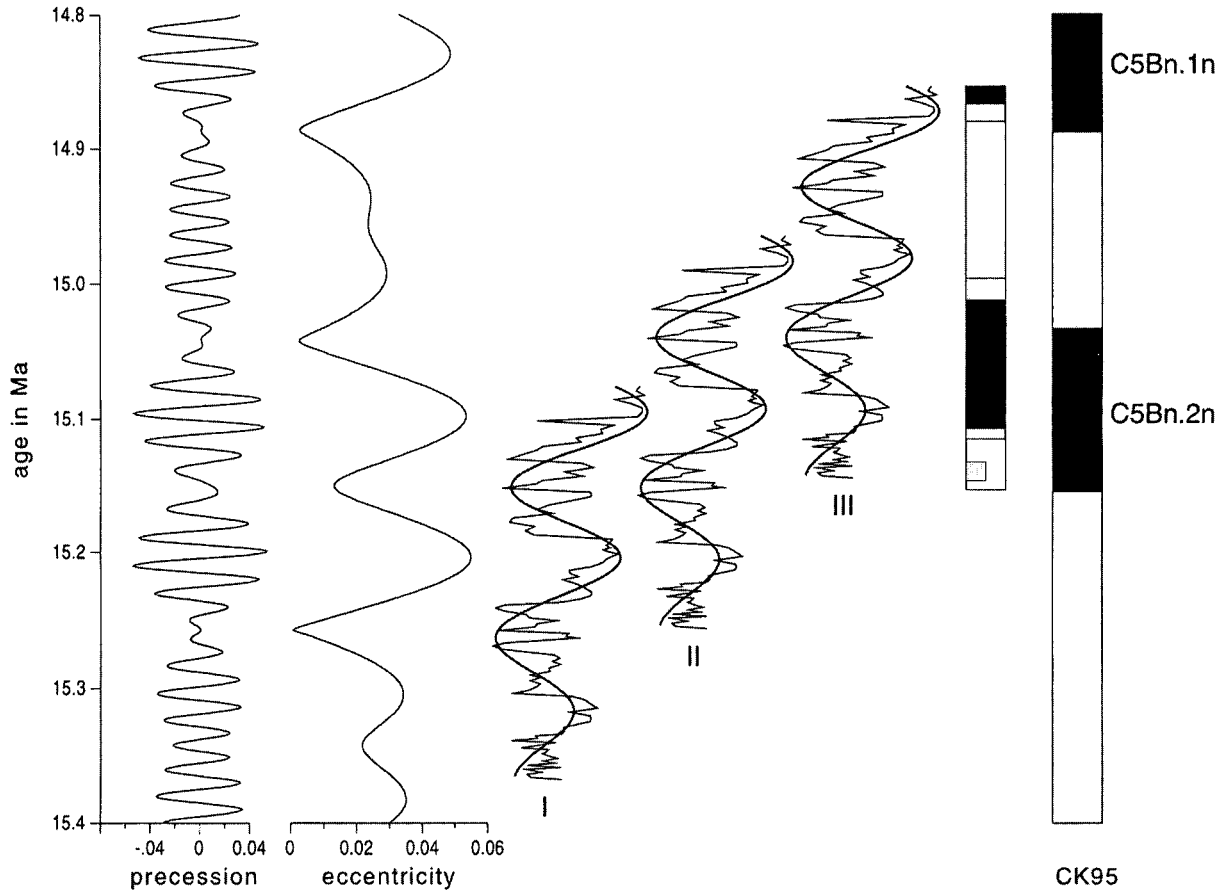

Figure 12. Precession and eccentricity according to La90. The carbonate record (thin line) has been filtered (thick line) using a low-pass filter in the frequency domain. Magnetostratigraphy is correlated to CK95. The three most appropriate correlations of the carbonate record to La90 are shown (see text); our preferred correlation is option I.

Figura 12. Precesión y excentricidad segun la solución de Laskar (1990). El registro del contenido en carbonato (línea delgada) se ha filtrado (línea gruesa). La sucesión magnetoestratigráfica se ha correlacionado con la escala de tiempo de polaridad geomagnética. Las tres posibles correlaciones de la curva de carbonato con la escala de Laskar (1990) están representadas (ver el texto); la correlación más favorable es la opción I.

If we assume that a maximum in the carbonate record corresponds to a maximum in eccentricity, then different correlations can be made to the astronomical solutions of La90 (Fig. 12). The best fit is given by the oldest correlation, the younger correlations are less likely because the maxima in carbonate record do not fit well to the eccentricity curve. The older correlation suggests that the age of 14.8 Ma of C5Bn.1n(y) in CK95 is probably too young, but it would be in good agreement with the radiometric dating of Andreieff et al. (1976). If our correlation is correct we find ages of 15.33 Ma for C5Bn.2n(o), 15.23 Ma for C5Bn.2n(y) and 15.10 Ma for C5Bn.1n(o). Obviously, longer detailed carbonate records are needed to confirm these suggestions.

CONCLUSIONS

The paleomagnetic signal of the Armantes red-bed section is generally of good quality. The ChRM is determined by hematite as well as magnetite and/or maghemite. Even though these components do not always show the same polarity at the same level, it is possible to determine the polarity reversals with an accuracy of approximately 1 m which corresponds to ± 10 kyr. The relative contribution of hematite is strongly dependent on the lithology. In the limestones, hematite is the dominant carrier of the magnetisation, whereas the contribution of magnetite/maghimite is of major importance in the silts. The absolute contribution of hematite is higher in the silts than in the limestones.

The distinct cyclic alternation of pink/white limestones and red silts is magnetostratigraphically dated to have a periodicity of 111 kyr (Krijgsman et al., 1994). Spectral analysis of the astronomical solutions of La90 for the correlative time interval (14.5-15.5 Ma) shows two equal intensity peaks at 125 and 95 kyr, resulting in an average periodicity of 110 kyr for eccentricity. This is in excellent agreement with our magnetostratigraphic results and confirms the suggestion that the large-scale cyclicity in the Armantes section is related to the eccentricity cycle of the Earth's orbit. From a paleoclimatological point of view it is most likely that the large-scale maxima in carbonate content correspond to maxima in eccentricy, and the small-scale maxima in carbonate content to minima in precession.

The magnetostratigraphic results from this detailed study show that the interval between the three reversals covers two large-scale cycles, suggesting a duration of approximately 220 kyr whereas the corresponding duration according to CK95 is 267 kyr. Tentative correlations of the carbonate record to the eccentricity curve of La90 shows a best fit, which suggests that ages in CK95 are slightly (175 kyr) too young. Such difference between astronomical duration and the duration according to the GPTS has been observed before, and mainly depends on errors in the ages of the calibration points in the GPTS. Our best fit correlation is in good agreement with the radiometric dating of 15.0 ± 0.3 Ma (Andreieff et al., 1976).

Altogether, this study indicates that the conditions for constructing an APTS in the continental deposits of the Calatayud-Daroca basin are favourable. On the basis of this study, our future research will be directed to much longer and more detailed sections, which will provide the necessary information about the effects of both long-term variations (~400 and ~100 kyr eccentricity cycle) and short-term variations (precession cycle).

ACKNOWLEDGEMENTS

We thank Mark Dekkers and Frits Hilgen for useful discussions. Luc Lourens is greatfully acknowledged for providing the astronomical solutions of La90. Miguel Garcés kindly translated the abstract into Spanish. Ton Zalm and Marjan Reith assisted with the carbonate measurements and the TGA and X-ray experiments. This study was supported by the Netherlands Geosciences Foundation (GOA/NWO).

REFERENCES

Andreieff, P., Bellon, H., Westercamp, D., 1976. Chronométrie et stratigraphie comparée des édifices volcaniques et formations sédimentaires de la Martinique (Antilles francaises). Bull. B.R.G.M. 2e ser., 4, 335-346.

Baksi, A.K., 1993. A Geomagnetic Polarity Time Scale for the period 0-17 Ma, based on $^{40}Ar/^{39}Ar$ plateau ages for selected field reversals. Geoph. Res. Lett., 20, 1607-1610.

Berggren, W.A., Kent, D.V., Flynn, J.J., Van Couvering, J.A., 1985. Cenozoic geochronology., Geol. Soc. Am. Bull., 96, 1407-1418.

Berggren, W.A., Kent, D.V., Swisher III, C.C., Aubry, M.P., 1995. A revised Cenozoic geochronology and chronostratigraphy, SEPM Spec. Publ., 54: Geochronology Time Scale and Global Stratigraphic Correlation, 129-212.

Blodgett, R.H., 1988. Calcareous paleosols in the Triassic Dolores Formation, southwestern Colorado. Geol. Soc. Am. Spec. Pap., 216, 103-121.

Cande, S.C., Kent, D.V., 1992. A new Geomagnetic Polarity Time Scale for the Late Cretaceous and Cenozoic, J. Geoph. Res., 97, 13917-13951.

Cande, S.C., Kent, D.V., 1995. Revised calibration of the Geomagnetic Polarity Time Scale for the Late Cretaceous and Cenozoic. J. Geoph. Res., 100, 6093-6095.

Channell, J.E.T., Freeman, R., Heller, F., Lowrie, W., 1982. Timing of diagenetic hematite growth in red pelagic limestones from Gubbio (Italy), Earth Planet. Sci. Lett., 58, 189-201.

De Boer, P.L., Smith, D.G., 1994. Orbital forcing and cyclic sequences, Spec. Publs. Int. Ass. Sediment., 19, 1-14.

De Bruijn, H., 1965. Miocene Gliridae, Sciuridae and Eomydae (Rodentia, Mammalia from the Calatayud area, prov. Zaragoza, Spain) and their bearing on the biostratigraphy. PhD Thesis, Univ. Utrecht.

Dekkers, M.J., Linssen, J.H., 1989. Rockmagnetic properties of fine-grained natural low-temperature haematite with reference to remanence acquisition mechanisms in red beds. Geophys. J. Int., 99, 1-18.

Dekkers, M.J., 1988. Some rockmagnetic parameters for natural goethite, pyrrhotite and fine-grained hematite, Geologica Ultraiectina, 51, PhD thesis, University of Utrecht.

Dijksman, A.A., 1977. Geomagnetic reversals as recorded in the Miocene Red Beds of the Calatayud-Teruel Basin (Central Spain). Ph.D. Thesis, Univ. Utrecht.

Dunlop, D.J., 1971. Magnetic properties of fine particle hematite, Ann. Géophys., 27, 269-293.

Füchtbauer, H., 1988 (ed.). Sedimente und Sedimentgesteine. Sediment-Petrologie teil II. E. Schweizbart'sche Verl. Stuttgart, 1141.

Hay, R.L., Wiggins, B., 1980. Pellets, ooid, sepiolite and silica in three calcretes of the southwestern United States. Sedimentology, 27, 559-576.

Hilgen, F.J., 1991a. Astronomical calibration of Gauss to Matayama sapropels in the Mediterranean and implication for the Geomagnetic Polarity Time Scale. Earth and Planet. Sci. Lett., 104, 226-244.

Hilgen, F.J., 1991b. Extension of the astronomically calibrated (polarity) time scale to the Miocene/Pliocene boundary. Earth and Planet. Sci. Lett., 107, 349-368.

Hilgen, F.J., Krijgsman, W., Langereis, C.G., Lourens, L.J., Santarelli, A., Zachariasse, W.J., 1995. An astronomical (polarity) time scale for the late Miocene. Earth Planet Sci. Lett., 136, 495-510.

Krijgsman, W., Hilgen, F.J., Langereis, C.G., Zachariasse, W.J., 1994a. The age of the Tortonian/Messinian boundary. Earth Planet. Sci. Lett., 121, 533-547.

Krijgsman, W., Langereis, C.G., Daams, R., Van der Meulen, A.J., 1994b. Magnetostratigraphic dating of the middle Miocene climate change in the continental deposits of the Aragonian type area in the Calatayud-Teruel basin (Central Spain). Earth Planet. Sci. Lett., 128, 513-526.

Krijgsman, W., Garcés, M., Langereis, C.G., Daams, R., Van Dam, J., Van der Meulen, A.J., Agustí, J., Cabrera, L., 1996. A new chronology for the middle to late Miocene continental record in Spain. Earth Planet. Sci. Lett., 142, 367-380.

Langereis, C.G., Dekkers, M.J., 1992. Paleomagnetism and rock magnetism of the Tortonian-Messinian boundary stratotype at Falconara, Sicily. Phys. of the Earth and Plan. Int., 71, 100-111.

Laskar, J., 1990. The chaotic motion of the solar system: a numerical astimate of the size of the chaotic zones. Icarus, 88, 266-291.

Miller, K.G., Aubry, M.P., Kahn, M.J., Melillo, A., Kent, D.V., Berggren, W.A., 1985. Oligocene-Miocene biostratigraphy, magnetostratiography, and isotope stratigraphy of the western North Atlantic. Geology, 13, 257-261.

Roberts, D.H., Lehar, J., Dreher, J.W., 1987. Time series analysis with CLEAN. I. Derivation of a spectrum. Astron. J., 93 (4), 968-989.

Park, J., Oglesby, R.J., 1994. The effect of orbital cycles on Late and Middle Cretaceous climate: a comparative general circulation model study. In de Boer, P.L., D.G. Smith (eds.). Orbital forcing and cyclic sequences. Int. Assoc. Sedim. Spec. Publ., 19, 509-529.

Rohling, E., Hilgen, F.J., 1991. The eastern Mediterranean climate at times of sapropel formation: a review. Geol. and Mijnb., 70, 253-264.

Rossignol-Strick, M., 1983. African monsoons, an immediate climatic response to orbital insolation. Nature, 303, 46-49.

Roy, J.L., Park, J.K., 1972. Red beds: DRM or CRM?. Earth Planet. Sci. Lett., 17, 211-216.

Shackleton, N. J., Berger A., Peltier W.R., 1990. An alternative astronomical calibration of the lower Pleistocene time scale based on ODP site 667. Trans. R. Soc. Edinburgh Earth Sci., 81, 251-261.

Shackleton, N.J., Crowhurst, S., Hagelberg, T., Pisias, N.G., and Schneider, D.A., 1995. A new late Neogene time scale: Application to leg 138 sites, In N.G. Pisias, L.A. Mayer, T.R. Janecek, A. Palmer-Julson, T.H. Van Andel (eds.), Proc. ODP, Sci. Res., 138, 73-101.

Tauxe, L., Mullender, T.A.T., Pick, T., 1995. Potbellies, wasp-waists, and superparamagnetism in magnetic hysteresis, J. Geoph. Res., 571-583.

Tsuchi, R. (ed.) 1981. Neogene of Japan: its biostratigraphy and chronology. IGCP-114 International workshop on Pacific Neogene Biostratigraphy (Osaka), 1-138.

Valdes, P.J., Sellwood, B.W., Price, G.D., 1995. Modelling Late Jurassic Milankovitch climate variations. In M.R. House, A.S. Gale (eds.). Orbital forcing timescales and cyclostratigraphy. Geol. Soc. Spec. Publ., 85, 115-132.

Van den Ende, C., 1977. Palaeomagnetism of Permian red beds of the Dôme de Barrot (S. France). Ph.D. thesis, University of Utrecht.

Van der Meulen, A.J., Daams, R., 1992. Evolution of early-middle Miocene rodent faunas in relation to long-term paleoenvironmental changes. Paleogeogr., Paleoclimatol., Paleoecol., 93, 227-253.

Walker, T.R., Honea, R.M., 1969. Iron content of modern deposits in the Sonoran Desert: a contribution to the origin of red beds. Geol. Soc. Am. Bull., 80, 535-544.

Walker, T.R., Larson, E.E., Hoblitt, R.P., 1981. Nature and origin of hematite in the Moenkopi Formation (Triassic), Colorado Plateau: a contribution to the origin of magnetism in red beds. J. Geophys. Res. B, 86, 317-333.